Blocking neutrophil diapedesis prevents hemorrhage during thrombocytopenia

Carina Hillgruber,[1,3] Birgit Pöppelmann,[1] Carsten Weishaupt,[1] Annika Kathrin Steingräber,[1] Florian Wessel,[4] Wolfgang E. Berdel,[2] J. Engelbert Gessner,[5] Benoît Ho-Tin-Noé,[6] Dietmar Vestweber,[4] and Tobias Goerge[1,3]

[1]Department of Dermatology and [2]Department of Medicine A–Hematology and Oncology, University Hospital of Münster and [3]Interdisciplinary Center for Clinical Research (IZKF), University of Münster, 48149 Münster, Germany
[4]Department of Vascular Cell Biology, Max Planck Institute for Molecular Biomedicine, 48149 Münster, Germany
[5]Clinical Department of Immunology and Rheumatology, Molecular Immunology Research Unit, Hannover Medical School, 30625 Hannover, Germany
[6]French Institute of Health and Medical Research (INSERM) U1148–Paris 7 University, Xavier Bichat Hospital, 75877 Paris, France

Spontaneous organ hemorrhage is the major complication in thrombocytopenia with a potential fatal outcome. However, the exact mechanisms regulating vascular integrity are still unknown. Here, we demonstrate that neutrophils recruited to inflammatory sites are the cellular culprits inducing thrombocytopenic tissue hemorrhage. Exposure of thrombocytopenic mice to UVB light provokes cutaneous petechial bleeding. This phenomenon is also observed in immune-thrombocytopenic patients when tested for UVB tolerance. Mechanistically, we show, analyzing several inflammatory models, that it is neutrophil diapedesis through the endothelial barrier that is responsible for the bleeding defect. First, bleeding is triggered by neutrophil-mediated mechanisms, which act downstream of capturing, adhesion, and crawling on the blood vessel wall and require $G\alpha_i$ signaling in neutrophils. Second, mutating Y731 in the cytoplasmic tail of VE-cadherin, known to selectively affect leukocyte diapedesis, but not the induction of vascular permeability, attenuates bleeding. Third, and in line with this, simply destabilizing endothelial junctions by histamine did not trigger bleeding. We conclude that specifically targeting neutrophil diapedesis through the endothelial barrier may represent a new therapeutic avenue to prevent fatal bleeding in immune-thrombocytopenic patients.

CORRESPONDENCE
Tobias Goerge:
tobias.goerge@ukmuenster.de
OR
Dietmar Vestweber:
vestweb@mpi-muenster.mpg.de

Abbreviations used: BAL, bronchoalveolar lavage; BMC, BM cell; DSC, dorsal skinfold chamber; GPCR, G protein–coupled receptor; ICD, irritative contact dermatitis; ICV, immune complex–mediated vasculitis; ITP, immune thrombocytopenia; MPO, myeloperoxidase; PTX, pertussis toxin; RT, room temperature.

A pathological low platelet count, thrombocytopenia, may be the cause of fatal bleeding. Thrombocytopenia results from platelet disorders, such as immune thrombocytopenia (ITP), or is observed in patients subjected to chemotherapy or BM transplantation (Psaila and Bussel, 2007; Izak and Bussel, 2014). Interestingly, not all patients with low platelet counts suffer from tissue hemorrhage, indicating that cofactors are required for the induction of thrombocytopenic bleeding (Aledort et al., 2004). Previous studies reported that the absence of platelets per se is not sufficient to cause bleeding, and the inflammatory response was seen as an inductor of thrombocytopenic hemorrhage (Goerge et al., 2008; Ho-Tin-Noé et al., 2011). Further work showed that degranulated platelets could not prevent intratumor hemorrhage, suggesting a possible link to granule release (Ho-Tin-Noé et al., 2008). More recently, the role of platelet immunoreceptor tyrosine activation motif (ITAM) signaling was identified to preserve vascular integrity during inflammation (Boulaftali et al., 2013). However, the mechanisms causing the loss of vascular integrity and leading to fatal inflammatory bleeding are still not identified, although interference with these might be of therapeutic benefit.

We observed that during thrombocytopenia, inflammation tips the balance toward hemorrhage (Goerge et al., 2008) and here speculate that this phenomenon results from inflammatory leukocyte–vessel wall interaction. Neutrophilic granulocytes, the major effector cells of the acute inflammatory response, are recruited

The Rockefeller University Press $30.00
J. Exp. Med. 2015 Vol. 212 No. 8 1255–1266
www.jem.org/cgi/doi/10.1084/jem.20142076

The Journal of Experimental Medicine

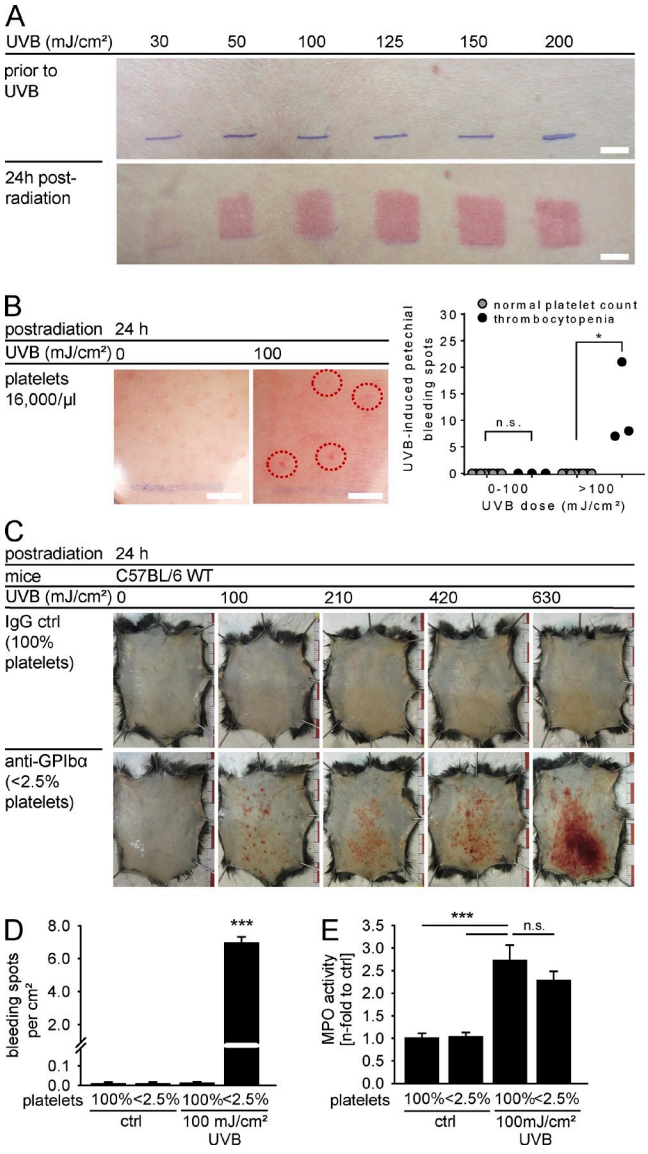

Figure 1. UVB-induced inflammation leads to cutaneous bleeding during thrombocytopenia. (A) Phototesting of a thrombocytopenic patient for individual UVB tolerance. Representative photographs of back skin area before UVB exposure (top) and 24 h after UVB exposure (bottom). Limited to irradiated square fields (1.5 cm × 1.5 cm), erythema developed within 24 h after exposure. (B) Representative close-up views of petechial bleeding from a thrombocytopenic patient 24 h after UVB radiation indicated with red dotted circles. Quantification of petechial bleeding in UVB-radiated square fields (1.5 cm × 1.5 cm) of three different thrombocytopenic patients compared with control subjects (n = 10). *, $P < 0.05$ versus normal platelet count. (A and B) Bars: (A) 1 cm; (B) 0.5 cm. (C) Representative prepared back skins of thrombocytopenic mice (<2.5% platelets; bottom) in response to the indicated UVB doses at 24 h after radiation time. (D) Quantification of cutaneous bleeding spots 24 h after single-dose UVB radiation (100 mJ/cm²). (E) UVB induced cutaneous neutrophil infiltration as measured by MPO activity. Data are presented as mean values ± SEM of n = 12 mice per group, verified in at least three independent experiments. ***, $P < 0.001$; n.s., not significant.

in a multistep process consisting of chemoattraction, selectin-mediated rolling, and integrin-mediated firm adhesion to the endothelium (Ley et al., 2007). Upon arrest, neutrophils get further activated by outside-in signaling, which initiates the transmigration through the endothelial layer (Faull and Ginsberg, 1996; Abram and Lowell, 2009). Strong and migration-competent interactions of neutrophils with endothelial cells, especially the activation of leukocyte integrins, depend on $G\alpha_i$ signaling (Spangrude et al., 1985; Rudolph et al., 1995). In this way, the $G\alpha_{i2}$ subunit of G protein–coupled receptors (GPCRs) is essential for cutaneous and pulmonary neutrophil extravasation (Wiege et al., 2013). Recently, it was shown that neutrophil interactions with endothelial cells trigger the dephosphorylation of Y731 in the cytoplasmic domain of VE-cadherin, which is required for proper diapedesis through the endothelial barrier (Wessel et al., 2014).

Here, we addressed these questions: how does inflammation trigger hemorrhage upon thrombocytopenia and what molecular mechanisms could be involved and serve as targets for preventing this defect? Thrombocytopenic patients exposed to UV light develop cutaneous petechial bleeding (Carbo et al., 2009). Indeed, we could observe this phenomenon called purpura solaris in thrombocytopenic patients phototested for UVB tolerance (UVB = UV light of 280–320-nm wavelength). In analogy, thrombocytopenic mice subjected to UVB radiation showed dose-dependent development of cutaneous bleeding. We found that depletion of neutrophils in thrombocytopenic mice completely blocked bleeding in the skin of these mice. In addition, we found that β_2 integrin–deficient $CD18^{-/-}$ mice (Wilson et al., 1993) were completely protected from petechial hemorrhage during thrombocytopenia. Moreover, by interference with $G\alpha_i$-mediated neutrophil recruitment, we were able to prevent both cutaneous and severe pulmonary hemorrhage during thrombocytopenia. Importantly, genetically modified mice expressing a Y731F mutant of VE-cadherin, known to inhibit neutrophil diapedesis, showed reduced tissue hemorrhage. Thus, blocking neutrophil diapedesis represents a promising target for preventing hemorrhage in thrombocytopenic patients.

RESULTS

UVB-induced inflammation leads to skin hemorrhage during thrombocytopenia in humans and in mice

Inflammation leads to bleeding during thrombocytopenia. Here, we studied UVB tolerance in patients suffering from ITP and in control subjects. Thrombocytopenic patients (<31,000 platelets/µl; skin type I–II according to Fitzpatrick classification) phototested for individual UVB tolerance showed 24 h later a dose-dependent mild erythema (Fig. 1 A) and the development of petechial bleeding spots at UVB doses >100 mJ/cm² (Fig. 1 B). Petechial bleeding was never observed in control subjects or nonirradiated areas of the thrombocytopenic patients. To characterize the underlying mechanism, we investigated UVB-radiated mice in a model of ITP (Nieswandt et al., 2000; Goerge et al., 2008). Although mice with full platelet count showed mild erythema, thrombocytopenic

mice dose-dependently developed cutaneous hemorrhage in the form of petechiae (Fig. 1 C). Bleeding spots per square centimeter were determined to quantify hemorrhage (Fig. 1 D). Similar to observations from the patients, petechial bleeding did not occur in nondepleted mice nor in nonirradiated thrombocytopenic mice. Analyzing tissue infiltration via the neutrophil-specific enzyme myeloperoxidase (MPO) revealed a significant neutrophil influx into UVB-radiated murine skin (Fig. 1 D). In summary, we observe that in the absence of platelets, UVB radiation provokes cutaneous bleeding (WHO bleeding grade I; Matzdorff et al., 2014) in humans and in mice.

Immune complex–mediated vasculitis (ICV)– and irritative contact dermatitis (ICD)–induced thrombocytopenic skin hemorrhage is accompanied by altered edema formation and neutrophil infiltration

Further experiments were performed in ICV and ICD, previously used for the study of petechial bleeding during thrombocytopenia (Goerge et al., 2008; Boulaftali et al., 2013). In analogy to UVB experiments, inflamed platelet-depleted mice developed overt cutaneous hemorrhage (Fig. 2 A). The bleeding area was strictly limited to the sites of inflammation and was never observed in mice with full platelet count or in noninflamed skin of thrombocytopenic mice. In previous work, the cellular culprit and the mechanism leading to thrombocytopenic bleeding could not be identified (Goerge et al., 2008). Here, we demonstrate that edema formation and neutrophil infiltration were significantly altered during thrombocytopenia (Fig. 2 B). Increase of biopsy weight was reduced by 30.0 ± 2.1% (ICV) or 30.8 ± 3.9% (ICD), and MPO activity was decreased by 42.7 ± 1.9% (ICV) or 59.7 ± 4.3% (ICD). Histological analysis of ICV biopsies confirmed prominent leukocyte infiltration in control mice, whereas red blood cells dominated the tissue in thrombocytopenic samples (Fig. 2 C). In summary, these data indicate that platelets both facilitate leukocyte extravasation to the inflamed skin and prevent hemorrhage.

Thrombocytopenic bleeding is not induced by vascular permeability per se

It may be speculated that increased vascular permeability might be sufficient to cause thrombocytopenic bleeding. Therefore, strong vascular leakage was induced in thrombocytopenic mice by intradermal injection of histamine. PBS injections served as negative controls. As shown in Fig. 3 A, histamine induced massive Evans blue leakage. The assay was repeated without the dye for better visibility of putative hemorrhage. However, in both assays substantial increase of vascular leakage, as measured by edema formation and Evans blue leakage, did not lead to any bleeding, in contrast to what was observed in ICV (Fig. 3 B). Thus, increased permeability per se is not sufficient to induce hemorrhage during thrombocytopenia.

Thrombocytopenic bleeding depends on neutrophil–endothelial cross talk

As we observed an altered neutrophil infiltration into the inflamed skin of platelet-depleted mice (Fig. 2 B), we sought to

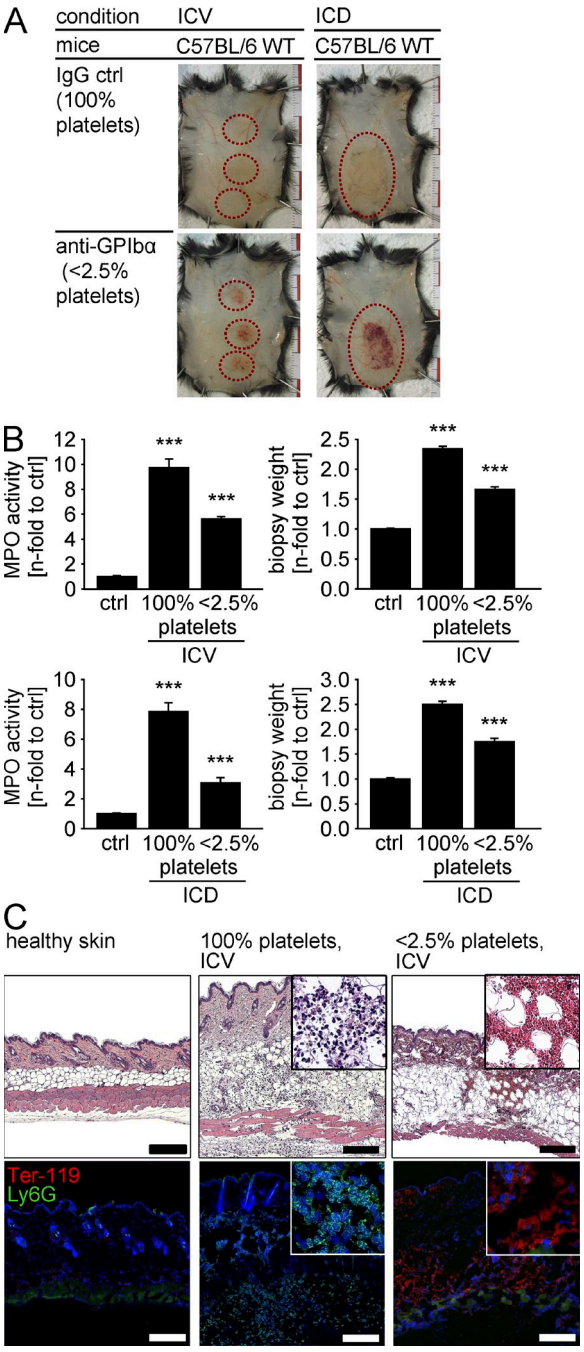

Figure 2. Development of thrombocytopenic hemorrhage is accompanied by altered edema formation and leukocyte recruitment during ICV and ICD. (A) Representative photographs of prepared back skins 4 h after ICV or ICD induction indicating cutaneous bleeding at inflammatory sites (red dotted circles) of thrombocytopenic mice compared with control mice. (B) Edema formation and MPO activity in platelet-depleted mice compared with control mice. Results are presented as mean values ± SEM of $n = 8–12$ mice per group from at least three independent experiments. ***, $P < 0.001$; n.s. not significant. (C) Histological analysis of mouse skin by H&E staining and immunofluorescent staining for erythroid Ter-119 and neutrophilic Ly6G. Healthy skin (left) served as a control. Fourfold magnified insets are shown. Microscopic images are representative of at least three independent stainings of at least 6 mice per group. Bars, 200 µm.

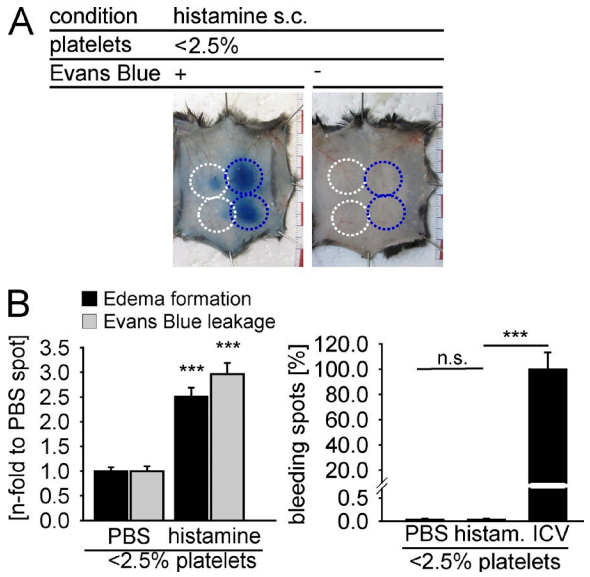

Figure 3. Vasodilatation per se is not required for induction of thrombocytopenic hemorrhage. (A) Representative photographs of prepared back skins of thrombocytopenic mice 4 h after subcutaneous histamine injection (blue dotted circles). White dotted circles indicate the area of PBS control injection. (B) Quantification of edema formation, Evans blue leakage, and petechial bleeding spots reveal histamine-induced strong vascular leakage but no cutaneous hemorrhage. The ICV bar indicating bleeding spots serves as a reference ($n \geq 4$ mice per group of two independent experiments). Mean ± SEM. ***, $P < 0.001$; n.s., not significant.

prevent thrombocytopenic bleeding by blocking neutrophil recruitment. Remarkably, upon depletion of granulocytes (anti–Gr-1) before ICV induction, there is virtually no bleeding detectable in inflamed thrombocytopenic mice compared with control animals (Fig. 4 A). Similar results were obtained by specific Ly6G depletion, thus identifying neutrophilic granulocytes as the relevant effector cells inducing thrombocytopenic hemorrhage during inflammation.

To investigate whether the mere presence of neutrophils is sufficient for the induction of bleeding or whether a more specific interaction of neutrophils with the vascular wall is required, we analyzed ICV-challenged thrombocytopenic mice while targeting successive steps of leukocyte recruitment. When using blocking antibodies to the chemoattractant KC, analyzing P-selectin knockout mice ($pSel^{-/-}$) or β_2 integrin–deficient mice ($CD18^{-/-}$), or using anti-CD11b antibodies, we observed a significant reduction in inflammatory bleeding during thrombocytopenia (Fig. 4, A and B [left]). As expected, interference with these successive steps of leukocyte recruitment resulted in significantly decreased neutrophil infiltration and edema formation (Fig. 4 B, middle and right). Of note, these findings were confirmed for the UVB and ICD model (Fig. 4, C and D).

Thrombocytopenic bleeding occurs at sites of leukocyte recruitment

So far, we could delineate that the presence of β_2 integrin–competent neutrophils is a prerequisite for thrombocytopenic bleeding in cutaneous inflammation; however, a direct proof for the interaction of leukocytes with the vessel wall is missing, and the kinetics of leukocyte recruitment are completely unknown. Therefore, we applied intravital microscopy in the dorsal skinfold chamber (DSC) that allows continuous observation of the inflammatory response in the cutaneous microcirculation. Upon ICV induction in the DSC, we continuously observed the multistep recruitment of fluorescently labeled leukocytes, as well as the development of petechial bleeding spots. In vivo images of bleeding spots and recruited leukocytes at indicated time points unravel that bleeding (Fig. 5 A, red arrowheads) occurs exactly and exclusively at the sites of extravasated leukocytes (Fig. 5 A, white arrowheads). Bleeding is never observed at sites without leukocyte recruitment. Numbers of both recruited leukocytes and bleeding spots increase over the time (Fig. 5 B, left), and there is a local correlation of leukocyte accumulation and the onset of thrombocytopenic bleeding (Fig. 5 B, right). About 90% of leukocytes are found within bleeding spots.

To prove the colocalization of neutrophil extravasation and red blood cell loss, we followed the leakage of fluorescently labeled beads (mimicking passive erythrocyte exit) during ICV in a DSC-bearing mouse. 4 h after ICV induction, mice with full platelet count showed massive leukocyte extravasation (Fig. 5 C, top, green) but no accumulation of fluorescent beads (Fig. 5 C, top, red). In contrast, we found obvious clustering of fluorescent beads at sites of recruited leukocytes in bleeding areas of thrombocytopenic mice (Fig. 5 C, middle). Quantification of microscopic photographs reveals that bleeding does only occur in the absence of platelets, accompanied by less leukocyte recruitment and a significant increase of bead accumulation compared with mice with full platelet counts (Fig. 5 D, top). Of note, blocking intraluminal crawling by administering an anti-CD11b antibody significantly reduces both leukocyte extravasation and development of petechial bleeding spots (Fig. 5, C and D, bottom). Thus, we formally demonstrate that in thrombocytopenic mice (but not platelet-sufficient mice), bead extravasation at a site of inflammation is concomitant with PMN extravasation but is not induced by just adhesion or rolling.

$G\alpha_{i2}$–dependent leukocyte transmigration is required for inflammatory hemorrhage during thrombocytopenia

The $G\alpha_{i2}$ subunit of GPCRs was described to be the essential $G\alpha$ subunit required for leukocyte extravasation during cutaneous and lung inflammation (Wiege et al., 2013). To investigate the role of leukocyte transmigration as a crucial step for thrombocytopenic bleeding, we blocked $G\alpha_i$-dependent signaling with pertussis toxin (PTX). Indeed, PTX treatment completely protected mice from skin bleeding during ICV (Fig. 6 A).

However, i.v. PTX application does not only affect GPCRs on leukocytes but also on endothelial cells. Therefore, we designed an adoptive transfer experiment. As $CD18^{-/-}$ mice are resistant to thrombocytopenic hemorrhage (Fig. 4), we transferred ex vivo treated WT leukocytes (PTX or vehicle)

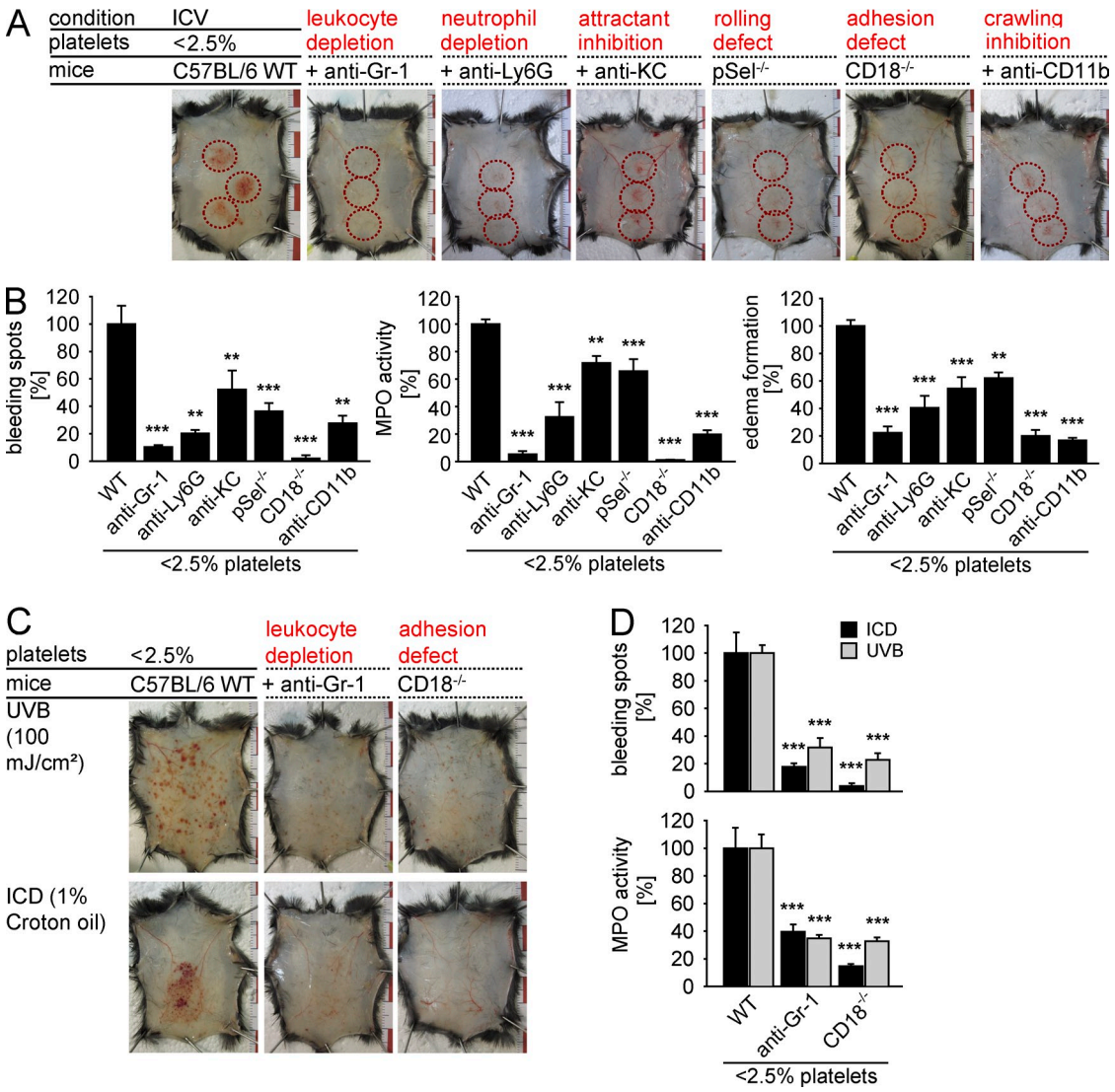

Figure 4. Neutrophil recruitment is required for induction of thrombocytopenic hemorrhage. (A) Representative photographs of prepared back skins of thrombocytopenic mice indicating petechial bleeding (red dotted circles) 4 h after ICV induction. Mice were either genetically modified or treated with antibodies to block neutrophil recruitment. (B) Analysis of bleeding spots per square centimeter, edema formation, and MPO activity of thrombocytopenic mice treated with anti-Gr-1, anti-Ly6G, or anti-KC antibodies (each 100 µg), and anti-CD11b antibodies (30 µg), as well as thrombocytopenic p-Selectin$^{-/-}$ and CD18$^{-/-}$ mice compared with thrombocytopenic WT controls. Results are presented as mean values ± SEM of $n \geq 6$ mice per group of at least two independent experiments. **, $P < 0.01$; ***, $P < 0.001$. (C) Thrombocytopenic mice were either exposed to a single dose of UVB (100 mJ/cm^2) or topically treated with 1% Croton oil (10 µl, in acetone). Representative photographs show prepared back skins 24 h after UVB radiation or 4 h after ICD induction. (D) Petechial bleeding and neutrophil infiltration in UVB- and ICD-challenged back skins of platelet-depleted WT mice compared with thrombocytopenic mice treated with anti-Gr-1 and thrombocytopenic CD18$^{-/-}$ mice ($n \geq 4$ mice per group of two independent experiments). Mean ± SEM. ***, $P < 0.001$.

into CD18$^{-/-}$ mice equipped with a DSC. This adoptive transfer allows the analysis of leukocyte recruitment after ex vivo modification of leukocyte function. The required dose of PTX for inhibition of neutrophil transmigration was determined in an in vitro assay (not depicted), and we proved the specific blockade of $G\alpha_i$-dependent neutrophil signaling in calcium influx assays (Fig. 6 B). Of note, WT leukocytes were able to induce petechial bleeding in a thrombocytopenic, ICV-challenged CD18$^{-/-}$ mouse, thus underlining the need of neutrophil–endothelial cross talk for induction of thrombocytopenic bleeding (Fig. 6 C, left). Moreover, ex vivo blockade of neutrophil $G\alpha_i$ signaling via PTX treatment completely prevented petechial bleeding (Fig. 6 C, right).

To visualize the fate of PTX-treated leukocytes compared with control cells at microscopic scale, we performed a two-color adoptive transfer experiment. Equal amounts of PTX (calcein green)- and control-treated (calcein red-orange) leukocytes were pooled and transferred into a CD18$^{-/-}$ mouse equipped with a DSC (Fig. 6 D). While control-treated leukocytes performed an ICV-induced multistep recruitment

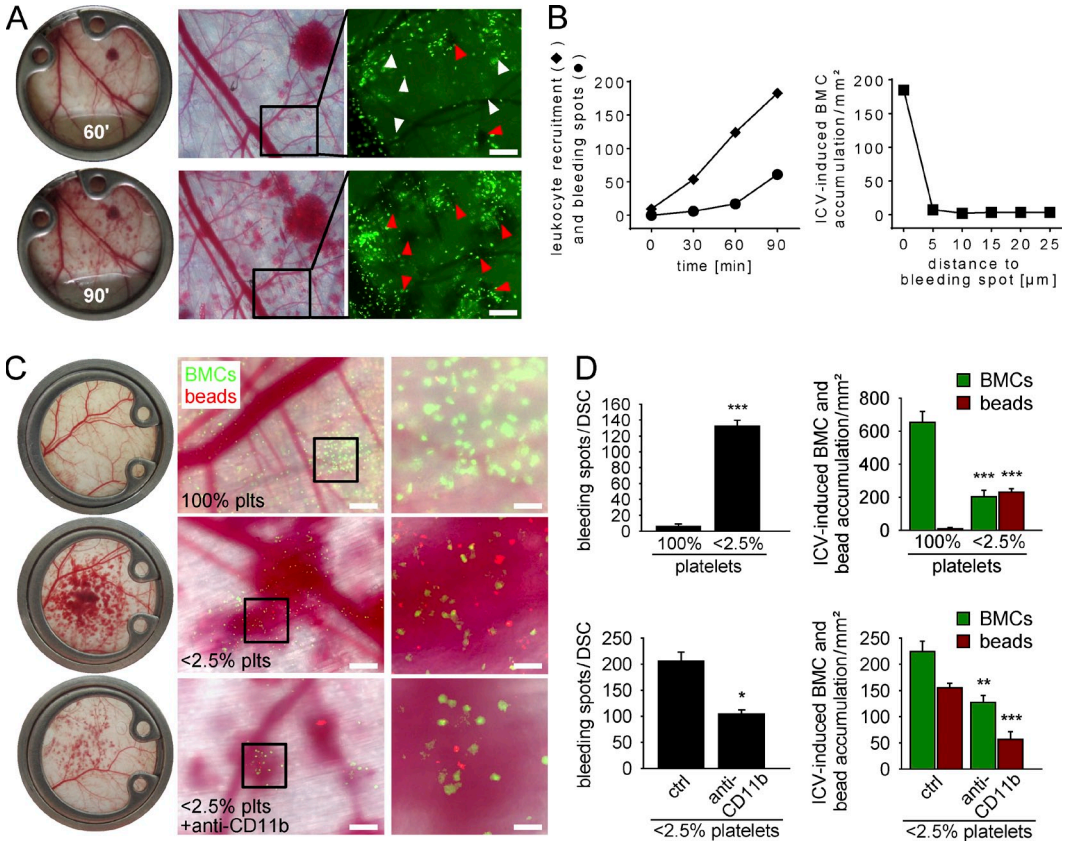

Figure 5. In vivo imaging reveals colocalization of neutrophil extravasation and red blood cell loss. (A) Calcein green–labeled WT BMCs were transfused into recipient WT mice before ICV induction on the backside of the DSC. Photographs show the development of petechial bleeding at the indicated time points during thrombocytopenia (top). One representative DSC's view field and magnified insets reveal development of petechial bleeding spots (red arrowheads) at sites of recruited leukocytes (white arrowheads). (B) Quantification results of leukocyte recruitment and petechial bleeding spots of equally exposed microscopic images. Left plot shows analysis of leukocyte recruitment (green fluorescence intensity) and counted bleeding spots over the time. Right plot illustrates the local distance of recruited leukocytes from bleeding spots (0 µm distance = leukocyte located within bleeding spot, >0 µm distance = leukocyte outside the bleeding spot). (A and B) Data are representative of three independent experiments with each one mouse per group. (C) WT BMCs and fluorescent beads (1 µm) were transfused into recipient WT mice before ICV induction on the backside of the DSC. Mice were treated with control IgG, platelet-depleting anti-GPIbα, or anti-GPIbα in combination with anti-CD11b. Representative macroscopic and microscopic images of a nondepleted mouse (100% plts), a thrombocytopenic mouse (<2.5% plts), and a thrombocytopenic mouse treated with anti-CD11b (<2.5% plts + anti-CD11b). Black boxes indicate the position of magnification. (A and C) Bars: (A and C [left]) 200 µm; (C, right) 50 µm. (D) Analysis of petechial bleeding spots, BMC recruitment, and fluorescent bead accumulation. Bleeding spots were quantified per DSC window, and recruited cells and accumulated beads were counted in areas of 500 µm × 500 µm and are depicted per square millimeter. Data are presented as mean values ± SEM of $n \geq 3$ mice per group of at least three individual experiments. *, $P < 0.05$; **, $P < 0.01$; ***, $P < 0.001$ each versus 100% platelets.

with initial rolling, firm adhesion, and extravasation to the inflamed skin, PTX-treated cells failed to adhere firmly. To further investigate the role of $G\alpha_i$ signaling for the onset of thrombocytopenic bleeding, we induced ICV in thrombocytopenic mice deficient for the $G\alpha_{i2}$ subunit, the essential subunit for pulmonary and cutaneous neutrophil extravasation (Wiege et al., 2013). Here, we confirm that $G\alpha_{i2}$ signaling significantly contributes to cutaneous thrombocytopenic bleeding (Fig. 6 E). In conclusion, the phenomenon of hemorrhage during thrombocytopenia is supported by $G\alpha_i$-mediated neutrophil extravasation.

Interference with $G\alpha_{i2}$-mediated neutrophil recruitment prevents lung hemorrhage during thrombocytopenia

Lung hemorrhage is a major clinical complication in ITP (Neunert et al., 2011; Rodeghiero et al., 2013; Matzdorff et al., 2014). Therefore, we investigated whether interference with neutrophil recruitment prevents pulmonary bleeding in inflamed thrombocytopenic mice. Indeed, although LPS-induced lung inflammation in thrombocytopenic mice led to massive lung hemorrhage, this bleeding was prevented by depletion of leukocytes as revealed by analysis of bronchoalveolar lavage (BAL; Fig. 7, A and B). As reported previously, platelets promote leukocyte recruitment during inflammation (Hara et al., 2010; Thornton et al., 2010; Jenne et al., 2013). Thus, fewer neutrophils were found in BAL of LPS-stimulated thrombocytopenic mice compared with inflamed mice with full platelet counts (Fig. 7 B). However, depletion of granulocytes protected thrombocytopenic mice from lung hemorrhage, as confirmed by histological analysis (Fig. 7 C). We then tested the role of $G\alpha_{i2}$ signaling in lung bleeding. Indeed,

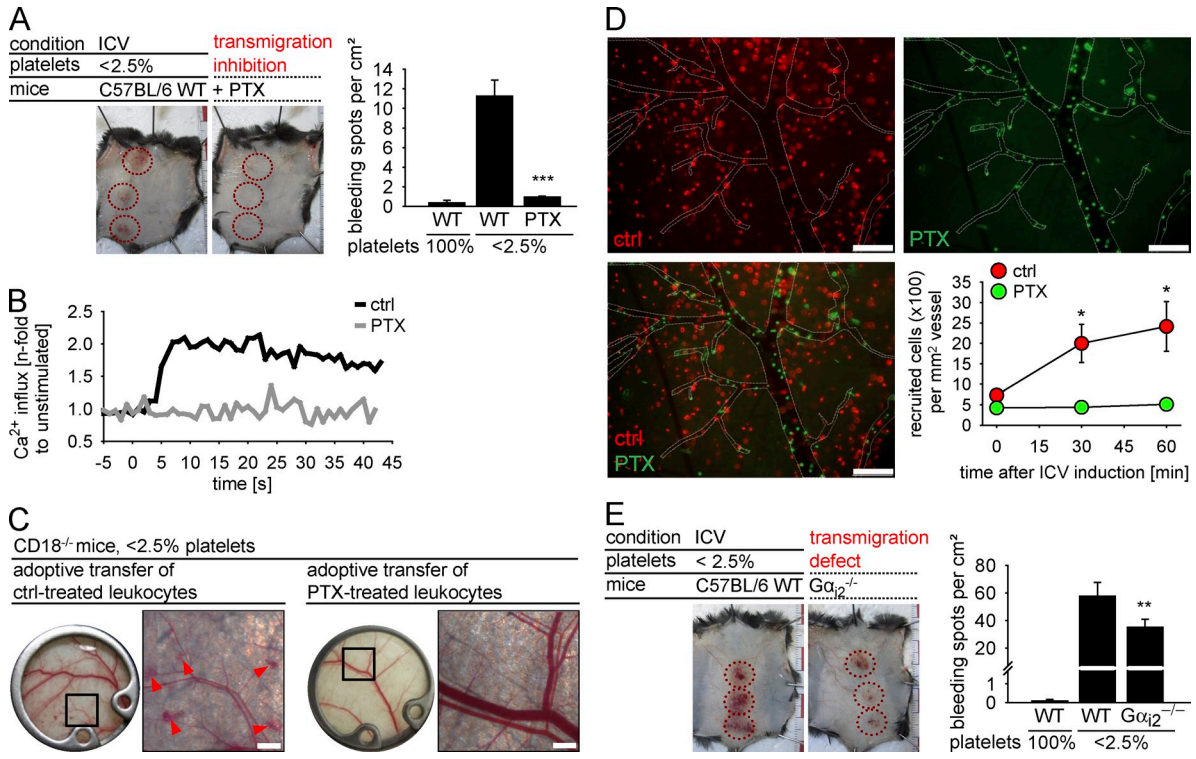

Figure 6. Blocking neutrophil $G\alpha_{i2}$ signaling protects thrombocytopenic mice from cutaneous hemorrhage. (A) Representative photographs and quantification of bleeding spots (red dotted circles) in PTX-treated mice compared with control mice (n = 6 mice per group of two independent experiments). Mean ± SEM. ***, P < 0.001. (B) Isolated WT BMCs were either treated with PTX or with vehicle. C5a-induced intracellular calcium influx in PTX-treated cells compared with control-treated cells. Results are representative of three individual experiments. (C) Isolated WT BMCs were either treated with PTX or with vehicle before transfusion into a DSC carrying $CD18^{-/-}$ recipient mice. Macroscopic and microscopic analysis of petechial bleeding after retransfusion of vehicle-treated WT leukocytes (red arrowheads) compared with retransfusion of PTX-treated leukocytes. Black boxes indicate the position of microscopic magnification. Photographs are representative of two independent experiments with each one mouse per group. (D) In vivo images of control (ctrl)- and PTX-treated WT BMCs in the microcirculation of a DSC carrying $CD18^{-/-}$ mouse. Quantification results of microscopic images are shown for one representative experiment of three independent experiments with each one mouse per group. Mean ± SEM. *, P < 0.05. (C and D) Bars: (C) 500 µm; (D) 200 µm. (E) Representative photographs and quantification of bleeding spots (red dotted circles) in $G\alpha_{i2}^{-/-}$ mice compared with WT mice (n = 6 mice per group of two independent experiments). Mean ± SEM. **, P < 0.01.

thrombocytopenic PTX-treated WT mice or $G\alpha_{i2}^{-/-}$ mice subjected to LPS-induced lung inflammation were protected from lung damage (Fig. 7 D). In conclusion, blocking neutrophil recruitment on the cellular level (Gr-1 depletion) or on the molecular level (PTX treatment, $G\alpha_{i2}^{-/-}$ mice) prevents severe lung hemorrhage (WHO bleeding grade IV) during thrombocytopenia.

Disruption of the endothelial barrier by neutrophils induces hemorrhage

Because neutrophil extravasation but not the disruption of the endothelial barrier by histamine led to thrombocytopenic hemorrhage, we hypothesized that bleeding requires a more robust opening of the barrier, which only leukocytes and not histamine can provide. Recently, we identified that the dephosphorylation of Y731 of VE-cadherin was selectively required for leukocyte extravasation but not for histamine-induced vascular permeability (Vestweber et al., 2014; Wessel et al., 2014). Analyzing platelet-depleted VE-cadherin–Y731F mutant mice in ICV, we found that these animals were indeed significantly protected from thrombocytopenic bleeding and neutrophil infiltration (Fig. 8, A and B) but showed an unaltered edema formation (Fig. 8 C). In line with these results, injection of C5a-activated neutrophils into the skin of $CD18^{-/-}$ mice failed to induce bleeding (Fig. 8, D and E), verifying that it is not simply the presence of activated neutrophils in the tissue, which would cause bleeding. In summary, preventing neutrophil diapedesis by either tightening the endothelial barrier or targeting neutrophil transmigratory activity leads to inhibition of blood loss in thrombocytopenia.

DISCUSSION

In the present manuscript we investigated the effector mechanisms leading to tissue bleeding during thrombocytopenia and demonstrate that neutrophils are the key players for the development of thrombocytopenic hemorrhage. We identify the diapedesis process consisting of $G\alpha_{i2}$-mediated neutrophil transmigratory activity and opening of the endothelial barrier

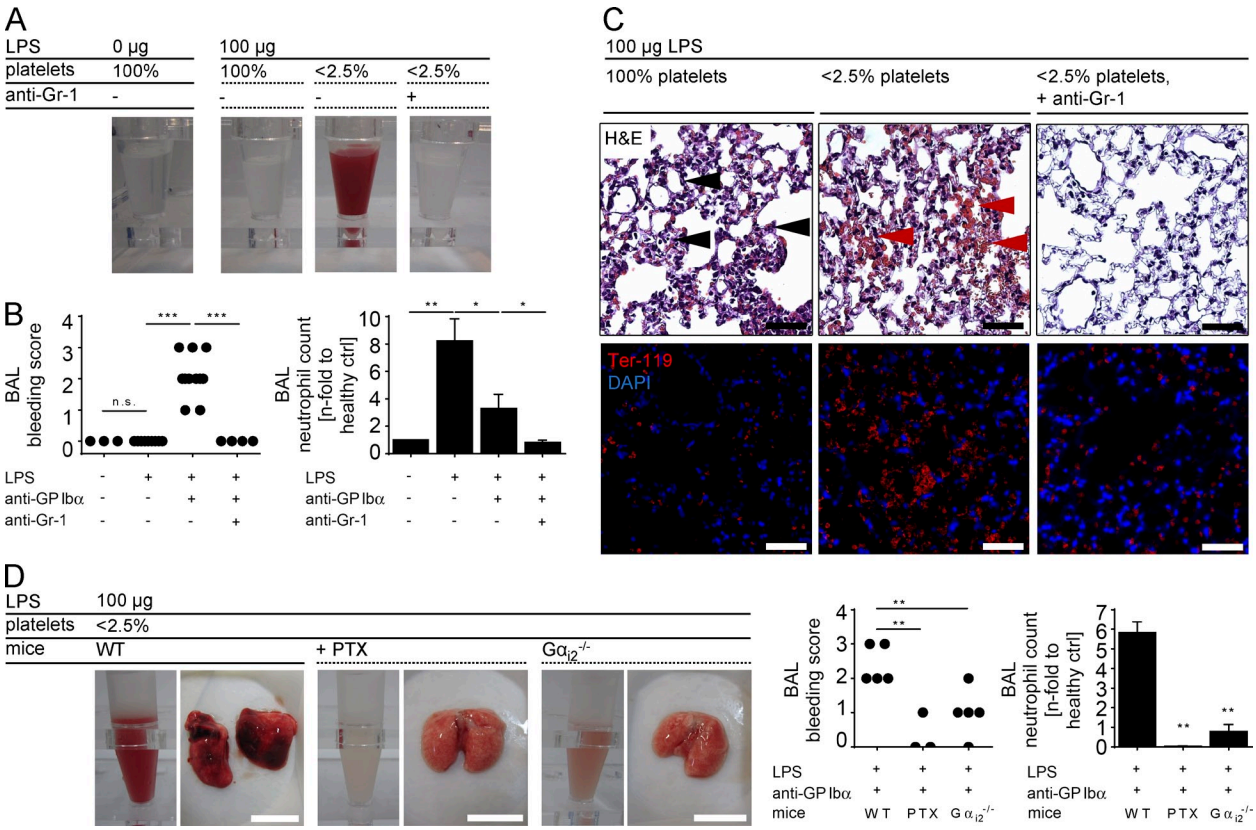

Figure 7. Blocking neutrophil $G\alpha_{i2}$ signaling protects thrombocytopenic mice from lung hemorrhage. (A) Representative photographs of BAL harvested 24 h after LPS-induced lung inflammation of a nondepleted mouse (100%), a thrombocytopenic mouse (<2.5%), and a thrombocytopenic mouse treated with anti-Gr-1 (<2.5% + anti-Gr-1) compared with a healthy control. (B) Analysis of BAL bleeding score and neutrophil counts ($n \geq 4$ mice per group of at least two individual experiments). Mean ± SEM. *, $P < 0.05$; **, $P < 0.01$; ***, $P < 0.001$; n.s., not significant. (C) Red blood cell accumulation (red arrowheads) and leukocyte recruitment (black arrowheads) as measured by H&E staining and immunofluorescent staining for erythroid Ter-119. Microscopic images are representative of three independent stainings of at least three mice per group. (D) Representative photographs and analysis of BAL and lung tissue harvested 24 h after LPS challenge in PTX-treated WT mice and $G\alpha_{i2}^{-/-}$ mice compared with control mice ($n \geq 3$ mice per group of one to two experiments). Mean ± SEM. **, $P < 0.01$. (C and D) Bars: (C) 50 µm; (D) 1 cm.

via VE-cadherin as an important step inducing thrombocytopenic hemorrhage in several models of inflammation. Our study suggests interference with neutrophil diapedesis as a novel therapeutic avenue to prevent bleeding in thrombocytopenia.

We found that neutrophils are the cellular inducers of thrombocytopenic bleeding (Fig. 4). This is in line with the fact that these leukocytes are the first cells infiltrating into inflammatory skin (Schubert et al., 1989; Sylvestre and Ravetch, 1994; Sindrilaru et al., 2007) and represent the key players for induction of cutaneous ICV (Feld et al., 2012). Moreover, in vivo imaging in the DSC (Lehr et al., 1993; Jain et al., 2002; Goerge et al., 2008; Ho-Tin-Noé et al., 2008; Feld et al., 2012) revealed the dependence of neutrophil recruitment and the onset of bleeding in space and time (Fig. 5), indicating the need of a specific neutrophil–endothelial cross talk for induction of thrombocytopenic hemorrhage. Different approaches to inhibit the interaction between the intruding neutrophils and the defending endothelium by interfering with P-selectin, β_2 integrin–mediated adhesion, and chemokine signaling led to reduced inflammatory bleeding during thrombocytopenia (Fig. 4). In addition, interference with $G\alpha_i$ signaling in neutrophils (a process known to be critical for neutrophil transmigration [Skokowa et al., 2005; Wiege et al., 2013]) by PTX treatment (Burns, 1988; Andreasen and Carbonetti, 2009; Bestebroer et al., 2010) or gene ablation (Rudolph et al., 1995) protected thrombocytopenic animals from neutrophil transmigration and cutaneous hemorrhage (Fig. 6). Thus, collectively, our results demonstrate that neutrophil diapedesis represents an essential step in inducing hemorrhage in thrombocytopenia.

The fact that neutrophils and their interactions with the endothelium were clearly required for hemorrhage raised the question of which mechanism would account for the loss of vascular integrity that facilitates bleeding. It is striking that neutrophil diapedesis but not leukocyte-independent interference with endothelial barrier integrity by histamine led to hemorrhage (Fig. 3). Thus, destabilization of endothelial junctions per se was not sufficient. This is in line with a previous study, which showed that tumor bleeding during thrombocytopenia was associated with neutrophil infiltration but not with VEGF-induced permeability (Ho-Tin-Noé et al., 2009).

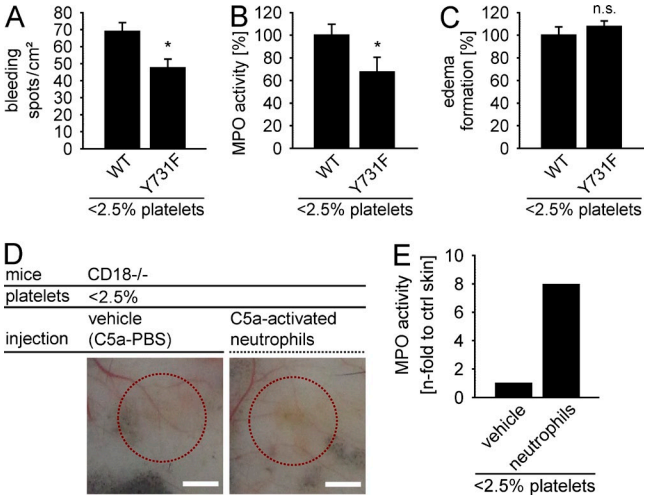

Figure 8. VE-cadherin–mediated opening of endothelial junctions and neutrophil transmigratory activity critically contribute to the induction of thrombocytopenic hemorrhage. (A) Analysis of cutaneous bleeding spots 4 h after ICV induction in thrombocytopenic WT mice compared with thrombocytopenic VEC-Y731F mice. (B) MPO activity in skin biopsies of VEC-Y731F mice compared with WT mice. (C) Edema formation in skin biopsies of VEC-Y731F mice compared with WT mice. Results are presented as mean values ± SEM of $n = 4$ mice per group of two independent experiments. *, $P < 0.05$; n.s., not significant. (D) C5a-activated neutrophils or control buffer were intradermally injected into the back skin of thrombocytopenic CD18$^{-/-}$ mice. Bleeding spots are indicated by red dotted circles. Representative photographs of injection sites. Bars, 2 mm. (E) Analysis of MPO activity in skin biopsies. Data are representative of three independent experiments with each one mouse per group.

Integrity of the endothelial barrier is dependent on the adhesive function of VE-cadherin, a major adhesion molecule at endothelial junctions (Vestweber, 2008). In line with this, leukocyte extravasation, as well as the induction of vascular permeability, is strongly inhibited upon stabilizing VE-cadherin function (Schulte et al., 2011). Thus, if permeability induction and leukocyte diapedesis both interfere with vascular integrity via addressing VE-cadherin, why then do only neutrophils but not permeability-inducing factors enhance bleeding? A recent finding provides the answer to this question: permeability-inducing factors such as histamine and VEGF target VE-cadherin in a different way than leukocytes (Vestweber et al., 2014; Wessel et al., 2014). We found that dephosphorylation of Y731 of VE-cadherin is exclusively involved in the extravasation of neutrophils but not relevant for the induction of vascular permeability (Wessel et al., 2014). Importantly, we show here that the Y731F mutation of VE-cadherin in appropriate knock-in mice could significantly reduce thrombocytopenic hemorrhage in ICV (Fig. 8). This establishes that neutrophil-triggered opening of endothelial junctions via addressing phosphorylation of Y731 of VE-cadherin destabilizes the endothelial barrier and leads to hemorrhage in thrombocytopenic mice.

Because bypassing diapedesis by directly injecting activated neutrophils into the skin did not induce thrombocytopenic hemorrhage, we conclude that it is not the mere presence of neutrophils in inflamed tissue, which would cause the bleeding. In summary, our results suggest that neutrophils cause hemorrhage while they are crossing through the endothelial barrier. Thus far, it can only be speculated how platelets via ITAM signaling (Boulaftali et al., 2013) are able to seal the damage induced by neutrophil diapedesis. The fact that platelets regulate vascular integrity (Nachman and Rafii, 2008) is supported by our finding that thrombocytopenic bleeding continues for the time of pathological low platelet counts (unpublished data) and stops directly when platelets are transfused (Goerge et al., 2008; Boulaftali et al., 2013).

Understanding the cellular and molecular mechanisms that lead to hemorrhage in thrombocytopenia is of utmost clinical interest. ITP patients may become resistant to various forms of ITP treatment, and specific antiinflammatory strategies without compromising the overall immune status of the patient are clearly needed (Neunert et al., 2011; Izak and Bussel, 2014; Matzdorff et al., 2014). We show here that inflammatory neutrophil–endothelial cross talk induces tissue bleeding during thrombocytopenia. We are aware that in the clinics bleeding may also occur without obvious signs of inflammation. We assume that petechial bleeding in the absence of overt inflammation might be caused by the presence of subclinical bacterial colonization leading to clinically undetected inflammation. However, so far we did not prove this hypothesis.

In thrombocytopenic patients, cutaneous bleeding (WHO bleeding grade I; Matzdorff et al., 2014) is obviously not as dreaded as pulmonary or cerebral hemorrhage (WHO bleeding grade IV; Matzdorff et al., 2014). Lung hemorrhage, a major clinical complication of ITP, may be life threatening for thrombocytopenic patients. Strikingly, by interference with pulmonary neutrophil transmigration, we were able to prevent thrombocytopenic mice from lung bleeding (Fig. 7). Thus, we demonstrate a pivotal role of neutrophil extravasation for the induction of severe thrombocytopenic lung hemorrhage and mechanistically explain the phenomenon of purpura solaris.

The treatment of bleeding in ITP patients is not yet satisfying. First, platelet transfusion is temporarily limited, and substitution has to be repeated in short episodes. Second, steroids, high-dose immunoglobulins, splenectomy, rituximab, or thrombopoietin-mimetic drugs do not show efficacy in all patients, the duration of response is variable, and there are multiple other limitations (Provan et al., 2010). We are aware that blocking innate immunity increases the risk of bacterial infection, which might require the use of antibiotics. Nevertheless, the present study demonstrates that specific interference with leukocyte diapedesis significantly prevents tissue hemorrhage during thrombocytopenia, thus representing a potential additional therapeutic avenue with an innovative mechanism of action for prevention of thrombocytopenic hemorrhage.

MATERIALS AND METHODS

Animals. 6–10-wk-old C57BL/6J (WT) mice were purchased from Harlan Laboratories, Inc., and were used as controls if not stated otherwise. Mice deficient in β_2 integrin (CD18$^{-/-}$; Wilson et al., 1993) and their littermates and P-selectin knockout mice (pSel$^{-/-}$; Mayadas et al., 1993) were bred and housed

under specific pathogen–free conditions in the animal facility of the University of Münster. Knock-in mice expressing a mutant of VE-cadherin (VEC-Y731F; Wessel et al., 2014) were bred and kept under specific pathogen–free conditions in a barrier facility at the Max Planck Institute for Molecular Biomedicine. Mice lacking $G\alpha_{i2}$ ($G\alpha_{i2}^{-/-}$; Rudolph et al., 1995) and their littermates were bred and kept in inhalator ventilation cages in the animal facility of Hannover Medical School. The genetic background of all used mouse lines is C57BL/6. All experiments have been approved by the local authorities (District Government and District Veterinary Office, Münster and Hannover, Germany).

Antibodies. The following antibodies were used: rabbit anti-BSA (MP Biomedicals), platelet-depleting monoclonal anti-GPIbα (R300; Emfret Analytics), leukocyte-depleting rat anti–mouse Ly6G and Ly6C (Gr-1, clone RB6-8C5; BD), neutrophil-depleting rat anti–mouse Ly6G (clone 1A8; BioLegend), anti–mouse CD11b (clone M1/70; BioLegend), monoclonal anti–mouse CXCL1/KC (R&D Systems), FITC rat anti–mouse Ly6G (clone 1A8; Miltenyi Biotec), and Biotin rat anti–mouse TER-119 (BioLegend).

Reagents. The following reagents were used: BSA (PAA Laboratories), hexadecyltrimethylammonium bromide (HTAB; Acros Organics), isoflurane (Forene 100%; Abbott), and recombinant mouse complement component 5a (C5a; R&D Systems). Calcein green, calcein red-orange, fluo-3 AM, FluoSpheres polystyrene microbeads orange (1 µm), and PTX were obtained from Life Technologies. LPS (from *Pseudomonas aeruginosa*), Evans blue, histamine, and tetramethylbenzidine (TMB) substrate were purchased from Sigma-Aldrich.

Platelet depletion. Concurrently with induction of inflammation (with exception of ICV), mice were i.v. injected either with 1.5 µg/g body weight of the well-established anti-GPIbα antibody (Bergmeier et al., 2000; Goerge et al., 2008; Petri et al., 2010) or with a nonimmune isotype control. For determination of platelet counts, mice were bled from the retro-orbital plexus under isoflurane anesthesia using heparinized microcapillaries. Platelets in whole blood were stained with FITC-labeled anti-αIIbβ3 antibody (clone Leo.F2; Emfret Analytics). Thrombocytopenia was validated by flow cytometry using a FACSCalibur (BD). Only mice with platelet counts ≤2.5% of normal WT count were included into experiments.

Leukocyte and neutrophil depletion. 24 h before induction of inflammation mice were intraperitoneally injected either with 100 µg anti–Gr-1 or anti-Ly6G or with a nonimmune isotype control. For determination of leukocyte or neutrophil counts, mice were bled from the retro-orbital plexus under isoflurane anesthesia using heparinized microcapillaries. After red blood cell lysis, leukocytes or neutrophils were stained with PE-labeled anti-neutrophil antibody (clone 7/4; Cedarlane). Depletion was validated by flow cytometry using a FACSCalibur.

UVB radiation. For UVB tolerance testing, patients (thrombocytopenic or control) were exposed to UVB after informed consent for this diagnostic procedure was obtained. This procedure fulfills the criteria expressed in the Helsinki declaration. Phototesting was performed using a source of UVB light (UV 801 BL; Waldmann). 24 h after a single dose of UVB (30–200 mJ/cm^2), photographs of patients' back skins were taken.

Shaved mice were exposed to a single dose of UVB (100–630 mJ/cm^2) using a bank of four sunlamps (UV-B TL40W/12; Philips) that emit wavelengths between 280 and 350 nm with a peak at 306 nm. Back skins of irradiated mice were analyzed 24 h after radiation.

ICV. In the case of anti-CD11b (30 µg) or anti-KC (100 µg) treatment, mice were i.v. injected with the antibody or an isotype control before inflammatory stimulation. ICV was induced by i.v. injection of BSA (150 µl, 1% in PBS) immediately followed by intradermal injection of anti-BSA antibody (20 µl, 1.5 µg/µl in PBS) under isoflurane anesthesia. To avoid bleeding from the needle tip, ICV was induced before platelet depletion. Mice were sacrificed after 4 h, and back skins were harvested and analyzed histologically for edema formation and MPO activity.

ICD. ICD was induced by application of 10 µl Croton oil (1% in acetone). Mice were sacrificed after 4 h, and back skins were harvested and analyzed histologically for edema formation and MPO activity.

Determination of MPO activity. Analysis of MPO activity was performed as described previously (Bradley et al., 1982). In brief, skin biopsies were shred in PBS, centrifuged (13,000 rpm, 10 min, room temperature [RT]), and resuspended in HTAB lysis buffer (1% in 50 mM potassium phosphate buffer). After centrifugation (13,000 rpm, 10 min, RT), the supernatant was assessed in triplicate for MPO activity by adding TMB substrate. Absorbance was measured at 630 nm for 20 min in a microplate reader (BioTek).

Permeability assay. Increased vascular permeability was achieved by intradermal injection of histamine (20 µl, 100 µM in PBS) under isoflurane inhalation. Evans blue (i.v. 150 µl, 0.5% in PBS) allowed visualization of vascular leakage. 4 h after histamine application mice were sacrificed, and back skin punch biopsies of 8-mm diameter were analyzed for edema formation and Evans blue leakage. After storage in formamide (24 h, RT) the supernatant was taken for OD measurement at 630 nm.

LPS-induced lung inflammation. Groups of mice were sedated with ketamine (80 mg/kg; Ceva) and xylazine (14 mg/kg; Ceva) and inoculated intranasally with 100 µg *P. aeruginosa* LPS or PBS as control. 10 min after intranasal application, platelets were depleted. 24 h later BAL was harvested by cannulating the trachea with an 18-gauge Angiocath, and lungs were lavaged five times with 1.0 ml cold sterile PBS. BAL was analyzed for infiltrated neutrophils using a flow cytometer. In some cases lungs were harvested and analyzed histologically.

Histology. Biopsies were either fixed in 4% formalin for paraffin embedding or in OCT matrix (NEG 50; Thermo Fisher Scientific) for cryostat sectioning. Paraffin-embedded specimens were stained with hematoxylin and eosin (H&E), and frozen specimens were stained for neutrophilic Ly6G and erythroid Ter-119. All samples were counterstained with DAPI and examined on an AxioImager.Z2 (Carl Zeiss) using 10× (numerical aperture 0.3) and 40× (numerical aperture 0.75) Plan-Neofluar magnification objectives. Images were analyzed with AxioVision software (version 4.8; Carl Zeiss).

FACS analysis of calcium influx. Neutrophils were isolated from whole BM by using the EasySep mouse neutrophil enrichment kit (#19762, STEMCELL Technologies). Isolated neutrophils were incubated with PTX (10 µg/ml) or vehicle for 60 min. Pretreated cells (10^6) were incubated with 10 µM of the calcium-sensing dye fluo-3 AM for 30 min, washed in PBS containing 1% fetal calf serum and 2 mM EDTA, resuspended in PBS containing $CaCl_2$ and $MgCl_2$, activated with C5a (10 ng/ml), and analyzed immediately by FACS. Data were evaluated with FlowJo software (Tree Star).

In vivo imaging of leukocyte recruitment. Mice were anesthetized by intraperitoneal injection of ketamine (80 mg/kg; Ceva) and xylazine (14 mg/kg; Ceva), and surgical preparation of DSCs was performed as described previously (Goerge et al., 2008; Feld et al., 2012). Mice were allowed to recover from surgery for 24 h. For in vivo microscopic observations, the DSC was attached to the microscope stage and intravital microscopy was performed on an epifluorescence microscope (AxioImager.Z2) using 2.5× (numerical aperture 0.075) and 10× (numerical aperture 0.3) Plan-Neofluar magnification objectives. Before intravital microscopy was performed in the DSC, 3×10^7 BM cells (BMCs), extracted from C57BL/6 donor mice, were labeled with calcein green (5 µg/ml) or calcein red-orange (10 µg/ml) and transferred into recipient mice by tail vein injection. Additionally, BMCs were incubated with PTX (10 µg/ml) or vehicle for 60 min. ICV was performed in the DSC as described previously (Goerge et al., 2008; Feld et al., 2012). Leukocyte recruitment was recorded by attached cameras (AxioCam MRm/MRc; Carl Zeiss), and data acquisition was performed with AxioVision software (version 4.8). For quantification of recruited BMCs, cells were counted in relation to vessel diameter.

To study the temporal dependence of leukocyte recruitment and the onset of bleeding during ICV in the DSC, we counted ICV-induced bleeding

spots and quantified leukocyte recruitment by measurement of the green fluorescent intensity (using the Adobe Photoshop histogram function) of equally exposed microscopic images (0, 30, 60, and 90 min after ICV induction). To study the local dependence of ICV-induced leukocyte recruitment and bleeding spots in the DSC, we determined the numbers of leukocytes both outside and inside the area of bleeding by analyzing view fields of 500 µm × 500 µm of equally exposed microscopic images (4 h after ICV induction). In addition, we analyzed the distance from extra-petechial leukocytes to the edge of the bleeding spot.

To formally demonstrate the colocalization of leukocyte recruitment and red blood cell loss during ICV in the DSC, thrombocytopenic mice additionally achieved 2.5×10^8 fluorescently labeled beads (1 µm, i.v.) 60 min after ICV induction in the DSC. Cell recruitment and bead leakage were followed over time, and macroscopic as well as microscopic photographs were taken. View fields of 500 µm × 500 µm of equally exposed microscopic images (4 h after ICV induction) were analyzed for leukocyte extravasation and bead accumulation. Bleeding spots were quantified per whole DSC window from macroscopic images.

Intradermal neutrophil transfer. Neutrophils were isolated from whole BM by using the EasySep mouse neutrophil enrichment kit. For transfer experiments, 10^6 activated WT neutrophils (C5a, 10 ng/ml) or vehicle (C5a-containing PBS) were immediately injected intradermally in the back skin of $CD18^{-/-}$ mice. To avoid bleeding from the needle tip, neutrophils were injected 10 min before platelet depletion. Mice were sacrificed after 4 h, and back skins were harvested and analyzed for petechial bleeding and MPO activity.

Statistical analysis. Data are presented as mean ± SEM. Statistical evaluation and plotting were performed in SigmaPlot (version 11.0; Systat Software Inc.) or Prism (GraphPad Software). If two groups were compared, Student's *t* test (if normally distributed) or Mann-Whitney rank sum test was performed. One-way ANOVA (if normally distributed) or Kruskal-Wallis ANOVA on Ranks was used if more than two groups were analyzed. Values of *, $P < 0.05$; **, $P < 0.01$; and ***, $P < 0.001$ were regarded as statistically significant.

This work was supported by the fund of the Interdisciplinary Center for Clinical Research (IZKF, Münster, Germany; Goe2/023/10 to T. Goerge), Deutsche Forschungsgemeinschaft (GO1360/4-1 to T. Goerge; SFB 629 and SFB 1009 to D. Vestweber; DFG 892/11-1 to J.E. Gessner), Cells-in-Motion Cluster of Excellence EXC 1003–CiM (University of Münster, Germany; to T. Goerge, D. Vestweber, and W.E. Berdel), and by the DHU FIRE, USPC, and CORDDIM (to B. Ho-Tin-Noé).

The authors declare no competing financial interests.

Author contributions: C. Hillgruber performed the research, analyzed and interpreted data, and wrote the manuscript; B. Pöppelmann, C. Weishaupt, and A.K. Steingräber performed the research and analyzed data; W.E. Berdel, B. Ho-Tin-Noé, J.E. Gessner, and F. Wessel provided tools and interpreted data; D. Vestweber provided tools, interpreted data, and contributed to writing the manuscript; T. Goerge designed the study, interpreted data, and wrote the manuscript.

Submitted: 4 November 2014
Accepted: 11 June 2015

REFERENCES

Abram, C.L., and C.A. Lowell. 2009. The ins and outs of leukocyte integrin signaling. *Annu. Rev. Immunol.* 27:339–362. http://dx.doi.org/10.1146/annurev.immunol.021908.132554

Aledort, L.M., C.P. Hayward, M.G. Chen, J.L. Nichol, and J. Bussel. ITP Study Group. 2004. Prospective screening of 205 patients with ITP, including diagnosis, serological markers, and the relationship between platelet counts, endogenous thrombopoietin, and circulating antithrombopoietin antibodies. *Am. J. Hematol.* 76:205–213. http://dx.doi.org/10.1002/ajh.20104

Andreasen, C., and N.H. Carbonetti. 2009. Role of neutrophils in response to *Bordetella pertussis* infection in mice. *Infect. Immun.* 77:1182–1188. http://dx.doi.org/10.1128/IAI.01150-08

Bergmeier, W., K. Rackebrandt, W. Schröder, H. Zirngibl, and B. Nieswandt. 2000. Structural and functional characterization of the mouse von Willebrand factor receptor GPIb-IX with novel monoclonal antibodies. *Blood.* 95:886–893.

Bestebroer, J., C.J. De Haas, and J.A. Van Strijp. 2010. How microorganisms avoid phagocyte attraction. *FEMS Microbiol. Rev.* 34:395–414. http://dx.doi.org/10.1111/j.1574-6976.2009.00202.x

Boulaftali, Y., P.R. Hess, T.M. Getz, A. Cholka, M. Stolla, N. Mackman, A.P. Owens III, J. Ware, M.L. Kahn, and W. Bergmeier. 2013. Platelet ITAM signaling is critical for vascular integrity in inflammation. *J. Clin. Invest.* 123:908–916. http://dx.doi.org/10.1172/JCI6515

Bradley, P.P., D.A. Priebat, R.D. Christensen, and G. Rothstein. 1982. Measurement of cutaneous inflammation: estimation of neutrophil content with an enzyme marker. *J. Invest. Dermatol.* 78:206–209. http://dx.doi.org/10.1111/1523-1747.ep12506462

Burns, D.L. 1988. Subunit structure and enzymic activity of pertussis toxin. *Microbiol. Sci.* 5:285–287.

Carbo, C., I. del Conde, and D. Duerschmied. 2009. Petechial bleeding after sunburn in a patient with mild thrombocytopenia. *Am. J. Hematol.* 84:523. http://dx.doi.org/10.1002/ajh.21321

Faull, R.J., and M.H. Ginsberg. 1996. Inside-out signaling through integrins. *J. Am. Soc. Nephrol.* 7:1091–1097.

Feld, M., T. Goerge, C. Hillgruber, A.K. Steingräber, M. Fastrich, V. Shpacovitch, and M. Steinhoff. 2012. α-1-Antitrypsin and IFN-γ reduce the severity of IC-mediated vasculitis by regulation of leukocyte recruitment in vivo. *J. Invest. Dermatol.* 132:2286–2295. http://dx.doi.org/10.1038/jid.2012.137

Goerge, T., B. Ho-Tin-Noe, C. Carbo, C. Benarafa, E. Remold-O'Donnell, B.Q. Zhao, S.M. Cifuni, and D.D. Wagner. 2008. Inflammation induces hemorrhage in thrombocytopenia. *Blood.* 111:4958–4964. http://dx.doi.org/10.1182/blood-2007-11-123620

Hara, T., K. Shimizu, F. Ogawa, K. Yanaba, Y. Iwata, E. Muroi, M. Takenaka, K. Komura, M. Hasegawa, M. Fujimoto, and S. Sato. 2010. Platelets control leukocyte recruitment in a murine model of cutaneous arthus reaction. *Am. J. Pathol.* 176:259–269. http://dx.doi.org/10.2353/ajpath.2010.081117

Ho-Tin-Noé, B., T. Goerge, S.M. Cifuni, D. Duerschmied, and D.D. Wagner. 2008. Platelet granule secretion continuously prevents intratumor hemorrhage. *Cancer Res.* 68:6851–6858. http://dx.doi.org/10.1158/0008-5472.CAN-08-0718

Ho-Tin-Noé, B., C. Carbo, M. Demers, S.M. Cifuni, T. Goerge, and D.D. Wagner. 2009. Innate immune cells induce hemorrhage in tumors during thrombocytopenia. *Am. J. Pathol.* 175:1699–1708. http://dx.doi.org/10.2353/ajpath.2009.090460

Ho-Tin-Noé, B., M. Demers, and D.D. Wagner. 2011. How platelets safeguard vascular integrity. *J. Thromb. Haemost.* 9:56–65. http://dx.doi.org/10.1111/j.1538-7836.2011.04317.x

Izak, M., and J.B. Bussel. 2014. Management of thrombocytopenia. *F1000Prime Rep.* 6:45. http://dx.doi.org/10.12703/P6-45

Jain, R.K., L.L. Munn, and D. Fukumura. 2002. Dissecting tumour pathophysiology using intravital microscopy. *Nat. Rev. Cancer.* 2:266–276. http://dx.doi.org/10.1038/nrc778

Jenne, C.N., R. Urrutia, and P. Kubes. 2013. Platelets: bridging hemostasis, inflammation, and immunity. *Int. J. Lab. Hematol.* 35:254–261. http://dx.doi.org/10.1111/ijlh.12084

Lehr, H.A., M. Leunig, M.D. Menger, D. Nolte, and K. Messmer. 1993. Dorsal skinfold chamber technique for intravital microscopy in nude mice. *Am. J. Pathol.* 143:1055–1062.

Ley, K., C. Laudanna, M.I. Cybulsky, and S. Nourshargh. 2007. Getting to the site of inflammation: the leukocyte adhesion cascade updated. *Nat. Rev. Immunol.* 7:678–689. http://dx.doi.org/10.1038/nri2156

Matzdorff, A., W. Eberl, A. Giagounidis, P. Imbach, I. Pabinger, and B. Wörmann. 2014. Immunthrombozytopenie—Onkopedia-Leitlinien Update: Empfehlungen einer gemeinsamen Arbeitsgruppe der DGHO, ÖGHO, SGH + SSH und GPOH. (In German). *Oncol. Res. Treat.* 37:6–25. http://dx.doi.org/10.1159/000356910

Mayadas, T.N., R.C. Johnson, H. Rayburn, R.O. Hynes, and D.D. Wagner. 1993. Leukocyte rolling and extravasation are severely compromised in P selectin-deficient mice. *Cell.* 74:541–554. http://dx.doi.org/10.1016/0092-8674(93)80055-J

Nachman, R.L., and S. Rafii. 2008. Platelets, petechiae, and preservation of the vascular wall. *N. Engl. J. Med.* 359:1261–1270. http://dx.doi.org/10.1056/NEJMra0800887

Neunert, C., W. Lim, M. Crowther, A. Cohen, L. Solberg Jr., and M.A. Crowther. American Society of Hematology. 2011. The American Society of Hematology 2011 evidence-based practice guideline for immune thrombocytopenia. *Blood.* 117:4190–4207. http://dx.doi.org/10.1182/blood-2010-08-302984

Nieswandt, B., W. Bergmeier, K. Rackebrandt, J.E. Gessner, and H. Zirngibl. 2000. Identification of critical antigen-specific mechanisms in the development of immune thrombocytopenic purpura in mice. *Blood.* 96:2520–2527.

Petri, B., A. Broermann, H. Li, A.G. Khandoga, A. Zarbock, F. Krombach, T. Goerge, S.W. Schneider, C. Jones, B. Nieswandt, et al. 2010. von Willebrand factor promotes leukocyte extravasation. *Blood.* 116:4712–4719. http://dx.doi.org/10.1182/blood-2010-03-276311

Provan, D., R. Stasi, A.C. Newland, V.S. Blanchette, P. Bolton-Maggs, J.B. Bussel, B.H. Chong, D.B. Cines, T.B. Gernsheimer, B. Godeau, et al. 2010. International consensus report on the investigation and management of primary immune thrombocytopenia. *Blood.* 115:168–186. http://dx.doi.org/10.1182/blood-2009-06-225565

Psaila, B., and J.B. Bussel. 2007. Immune thrombocytopenic purpura. *Hematol. Oncol. Clin. North Am.* 21:743–759. http://dx.doi.org/10.1016/j.hoc.2007.06.007

Rodeghiero, F., M. Michel, T. Gernsheimer, M. Ruggeri, V. Blanchette, J.B. Bussel, D.B. Cines, N. Cooper, B. Godeau, A. Greinacher, et al. 2013. Standardization of bleeding assessment in immune thrombocytopenia: report from the International Working Group. *Blood.* 121:2596–2606. http://dx.doi.org/10.1182/blood-2012-07-442392

Rudolph, U., M.J. Finegold, S.S. Rich, G.R. Harriman, Y. Srinivasan, P. Brabet, G. Boulay, A. Bradley, and L. Birnbaumer. 1995. Ulcerative colitis and adenocarcinoma of the colon in $G\alpha_{i2}$-deficient mice. *Nat. Genet.* 10:143–150. http://dx.doi.org/10.1038/ng0695-143

Schubert, C., E. Christophers, O. Swensson, and T. Isei. 1989. Transendothelial cell diapedesis of neutrophils in inflamed human skin. *Arch. Dermatol. Res.* 281:475–481. http://dx.doi.org/10.1007/BF00510083

Schulte, D., V. Küppers, N. Dartsch, A. Broermann, H. Li, A. Zarbock, O. Kamenyeva, F. Kiefer, A. Khandoga, S. Massberg, and D. Vestweber. 2011. Stabilizing the VE-cadherin-catenin complex blocks leukocyte extravasation and vascular permeability. *EMBO J.* 30:4157–4170. http://dx.doi.org/10.1038/emboj.2011.304

Sindrilaru, A., S. Seeliger, J.M. Ehrchen, T. Peters, J. Roth, K. Scharffetter-Kochanek, and C.H. Sunderkötter. 2007. Site of blood vessel damage and relevance of CD18 in a murine model of immune complex-mediated vasculitis. *J. Invest. Dermatol.* 127:447–454. http://dx.doi.org/10.1038/sj.jid.5700563

Skokowa, J., S.R. Ali, O. Felda, V. Kumar, S. Konrad, N. Shushakova, R.E. Schmidt, R.P. Piekorz, B. Nürnberg, K. Spicher, et al. 2005. Macrophages induce the inflammatory response in the pulmonary Arthus reaction through $G\alpha_{i2}$ activation that controls C5aR and Fc receptor cooperation. *J. Immunol.* 174:3041–3050. http://dx.doi.org/10.4049/jimmunol.174.5.3041

Spangrude, G.J., F. Sacchi, H.R. Hill, D.E. Van Epps, and R.A. Daynes. 1985. Inhibition of lymphocyte and neutrophil chemotaxis by pertussis toxin. *J. Immunol.* 135:4135–4143.

Sylvestre, D.L., and J.V. Ravetch. 1994. Fc receptors initiate the Arthus reaction: redefining the inflammatory cascade. *Science.* 265:1095–1098. http://dx.doi.org/10.1126/science.8066448

Thornton, P., B.W. McColl, A. Greenhalgh, A. Denes, S.M. Allan, and N.J. Rothwell. 2010. Platelet interleukin-1α drives cerebrovascular inflammation. *Blood.* 115:3632–3639. http://dx.doi.org/10.1182/blood-2009-11-252643

Vestweber, D. 2008. VE-cadherin: the major endothelial adhesion molecule controlling cellular junctions and blood vessel formation. *Arterioscler. Thromb. Vasc. Biol.* 28:223–232. http://dx.doi.org/10.1161/ATVBAHA.107.158014

Vestweber, D., F. Wessel, and A.F. Nottebaum. 2014. Similarities and differences in the regulation of leukocyte extravasation and vascular permeability. *Semin. Immunopathol.* 36:177–192. http://dx.doi.org/10.1007/s00281-014-0419-7

Wessel, F., M. Winderlich, M. Holm, M. Frye, R. Rivera-Galdos, M. Vockel, R. Linnepe, U. Ipe, A. Stadtmann, A. Zarbock, et al. 2014. Leukocyte extravasation and vascular permeability are each controlled in vivo by different tyrosine residues of VE-cadherin. *Nat. Immunol.* 15:223–230. http://dx.doi.org/10.1038/ni.2824

Wiege, K., S.R. Ali, B. Gewecke, A. Novakovic, F.M. Konrad, K. Pexa, S. Beer-Hammer, J. Reutershan, R.P. Piekorz, R.E. Schmidt, et al. 2013. $G\alpha_{i2}$ is the essential $G\alpha_i$ protein in immune complex-induced lung disease. *J. Immunol.* 190:324–333. http://dx.doi.org/10.4049/jimmunol.1201398

Wilson, R.W., C.M. Ballantyne, C.W. Smith, C. Montgomery, A. Bradley, W.E. O'Brien, and A.L. Beaudet. 1993. Gene targeting yields a CD18-mutant mouse for study of inflammation. *J. Immunol.* 151:1571–1578.